Bull. Mater. Sci., Vol. 40, No. 3, June 2017, pp. 427–434
DOI 10.1007/s12034-017-1399-8

Electrochemical impedance studies of capacity fading of electrodeposited ZnO conversion anodes in Li-ion battery

G K KIRAN[1], TIRUPATHI RAO PENKI[2], N MUNICHANDRAIAH[2] and P VISHNU KAMATH[1,*]
[1]Department of Chemistry, Central College, Bangalore University, Bangalore 560 001, India
[2]Inorganic and Physical Chemistry, Indian Institute of Science, Bangalore 560 012, India
[*]Author for correspondence (vishnukamath8@hotmail.com)

MS received 9 June 2016; accepted 27 September 2016; published online 9 June 2017

Abstract. Electrodeposited ZnO coatings suffer severe capacity fading when used as conversion anodes in sealed Li cells. Capacity fading is attributed to (i) the large charge transfer resistance, R_{ct} (300–700 Ω) and (ii) the low Li^+ ion diffusion coefficient, D^+_{Li} (10^{-15} to 10^{-13} cm^2 s^{-1}). The measured value of R_{ct} is nearly 10 times higher and D^+_{Li} 10–100 times lower than the corresponding values for Cu_2O, which delivers a stable reversible capacity.

Keywords. ZnO; electrodeposition; Li-ion battery; anode; capacity fading.

1. Introduction

Transition metal oxides have attracted much attention as anode materials for Li-ion batteries. They are potential alternatives to carbon-based anodes, as they offer higher theoretical capacities. Among the many transition metal oxides, ZnO is an attractive candidate, as it is easy to prepare, low cost, and has a theoretical capacity of 978 mAh g^{-1}, which is higher than that of other oxides such as Cu_2O (375 mAh g^{-1}), CuO (670 mAh g^{-1}), NiO (718 mAh g^{-1}) and CoO (715 mAh g^{-1}) [1]. It is comparable to that of Co_3O_4 (890 mAh g^{-1}) [2], but offers cost advantages compared to the oxides of Co. ZnO was investigated earlier by many authors as an anode material for Li-ion batteries and was reported to suffer severe capacity fading within first five cycles.

In contrast, an oxide such as Cu_2O (*Pn*-3*m*, a = 4.2672 Å), which also offers cost advantages, delivers a stable capacity of 220 mAh g^{-1} in conversion anodes with an extended cycle life [3,4]. A recent investigation of electrodeposited Cu_2O coatings showed that the 200-oriented coating delivered a stable reversible capacity 16% higher than that delivered by the 111-oriented coating [5]. The higher deliverable capacity of the 200 crystal face of Cu_2O was attributed to its polar nature, whereby, it has a high surface energy and enhanced reactivity towards the incoming Li atoms. The 111 crystal face is non-polar, thermodynamically stable and relatively unreactive towards the incoming Li atoms.

ZnO in the wurtzite structure is unique in that its 001 crystal face is polar, atomically flat and does not reconstruct despite the high surface dipole moment [6]. Moreover, when deposited from a nitrate bath, the 001 crystal face of ZnO terminates with O^{2-} ions [7]. It is therefore expected that the 001 crystal face would be highly reactive towards incoming Li atoms in ZnO conversion anodes.

Several reasons are proposed for the observed capacity fading of ZnO anodes.

(i) The reduction of Li_2O to Li by Zn is not thermodynamically feasible. The large capacity observed in the first charge cycle corresponds to reduction of ZnO to Zn, followed by the formation of Zn–Li alloys; the former reaction which dominates the first charge cycle is irreversible and results in rapid capacity fading. The latter reaction is reversible and contributes to the small reversible capacity after the first charge [8].

(ii) Even with respect to alloy formation, it is proposed that the formation of highly crystalline alloys is responsible for further capacity fading. There are multiple alloys in the Zn–Li system and some of these actually slow down Li^+ transport during cycling. There are also suggestions that large volume changes during alloying produces changes in the microstructure which are deleterious to reversibility [9].

(iii) It is suggested that the high electrical resistivity of ZnO severely limits the rate capability of ZnO, leading to its poor performance under working conditions of the Li-ion batteries [10].

(iv) Despite the thermodynamic stability of Li_2O, its reduction in conversion electrodes is attributed to the high reactivity of metal nanoparticles formed after the first charge cycle. In case of ZnO anodes, it is suggested that after the first charge cycle, metallic zinc forms large crystallites with bulk-like properties and phase

separates [11]. Now the Zn is no more able to reduce Li_2O to Li. This results in accumulation of Li_2O and the matrix thickness leading to drop in conductivity [12].

There are many approaches for the remediation of ZnO for Li-battery applications, which include (i) synthesis of nanostructured ZnO followed by carbonation [13] or functionalization by Au nanoparticles [14], (ii) use of porous composites of $ZnO/ZnAl_2O_4$ which improves Li^+ transport, while simultaneously alleviating the problems associated with large volume changes during Li insertion [10], and (iii) use of highly conducting substrates to alleviate the problem of poor conductivity [15]. The use of fine particle ZnO obtained by ball milling shows no improvement in cyclability [9].

In this work, we examine if the problem of capacity fading of ZnO anodes can be addressed by enriching the anode with the polar 001 crystal face by fabricating oriented ZnO coatings.

Despite numerous suggestions that the observed capacity fading of ZnO anodes is due to the poor conductivity of ZnO, there are only limited reports of impedance measurements and even these are of either pristine anodes prior to cycling [16] or after complete lithiation [17]. ZnO anodes are generally fabricated by blending ZnO in conducting graphite and polymer binders. Any measurement performed on these conventional Li cells would correspond to the behaviour of the composite material taken as a whole. This necessitates a detailed exploration of a wide matrix of parameters involved in electrode fabrication to optimize the protocol for the best possible performance [16,17]. In this work, wurtzite ZnO coatings are fabricated by a single-step electrodeposition process [18] on a conducting stainless steel substrate, thereby obviating the need for any additives. The electrodeposited coatings were used as such in sealed half cells. Impedance measurements were performed and compared with similarly fabricated Cu_2O coatings used as a control. We report that the charge transfer resistance of ZnO anodes is 10 times higher and Li-diffusion coefficients are nearly two orders of magnitude lower compared to the Cu_2O anodes.

2. Experimental

Aqueous $Zn(NO_3)_2$ solutions (0.04–0.1 M) (Merck, India) were used for the electrodeposition of ZnO coatings. Ion-exchanged Type I water (Millipore Academic water purification system, specific resistance 18.2 MΩ cm) was used for the preparation of bath solutions. Electrodeposition was carried out using EG&G (PARC) Model Versastat IIA scanning potentiostat/galvanostat driven by M270 ECHEM software. A polycrystalline stainless steel disk (SS 304, area 1.57 cm^2) was used as cathode. A cylindrical Pt mesh (geometrical area 28 cm^2) was used as anode. The deposition was carried out at a constant potential of −0.9 V measured with respect to a saturated calomel electrode (SCE). ZnO coatings of different masses were obtained by varying the deposition time from 45 to 90 min and the temperature of the bath was maintained in the range of 50–70°C. Prior to electrodeposition, stainless steel electrodes were degreased with detergent and electrochemically cleaned.

All ZnO coatings were characterized by powder X-ray diffraction (PXRD) by mounting the electrode directly onto a Bruker aXS D8 Advance diffractometer (CuK α source $\lambda = 1.541$ Å). Data were recorded at a continuous scan rate of $1^\circ\ 2\theta\ min^{-1}$ and then rebinned into 2θ steps of 0.02°. Scanning electron micrographs (SEM) were obtained using JEOL Model JSM 6490LV microscope, by mounting ZnO-coated electrodes on conducting carbon tape and sputter coating with Pt to improve conductivity. The UV/Vis spectra (500–300 nm) were recorded with a Shimadzu Model UV-3100 UV/Vis/NIR scanning spectrometer fitted with an integrating sphere attachment Model ISR-3100, for spectral measurement in the diffuse reflectance mode. Transmission electron micrographs (TEM) were obtained from JEOL JEM-3010 electron microscope. The samples for TEM were prepared by sonicating the spent electrode material in ethanol and drop-casting a small volume onto a carbon-coated copper grid.

ZnO-coated SS 304 discs were used as negative electrodes for Li-on batteries. Li metal was used as a counter-cum-reference electrode. The electrolyte solution was 1 M $LiPF_6$ in ethylene carbonate, diethyl carbonate and dimethyl carbonate (2:1:2 v/v) (Chameleon). Swagelok-type cells were assembled in argon-filled MBRAUN glove box model UNILAB. The cells were cyclically tested on a CHI Model 408A instrument, galvanostatically at 100 μA current over a voltage range of 0.02–3.0 V. Electrochemical impedance spectra were recorded using CHI 6092C electrochemical analyzer. Impedance spectra were recorded before cycling and after the completion of 1, 5, 10, 20 and 25 charge–discharge cycles. Similar cells were fabricated using Cu_2O coatings as described elsewhere [5] and impedance spectra were recorded for these as well for use as control. The excitation signal was 5 mV (rms) at open-circuit voltage (3.0 V before charge–discharge cycle and 1.0 V after 25 charge–discharge cycles), and the frequency range was from 100 kHz to 10 mHz. All measurements were carried out at 22 ± 1°C.

3. Results and discussion

Electrodeposition is a simple, one-step soft chemical route to the fabrication of oxide coatings on conducting substrates [19,20]. Given the importance of ZnO for optoelectronic applications, there is extensive work on the electrodeposition of ZnO by Lincot and co-workers [21,22]. Additionally, ZnO can be electrodeposited with different out-of-plane orientations, by merely varying some of the deposition conditions [23]. A cohort of differently oriented ZnO coatings were fabricated (figure 1) by selecting the appropriate electrodeposition conditions reported earlier [18] and cycled in hermetically sealed Swagelok cells. These experiments were initiated to examine if the polar 001 crystal face of ZnO had a higher

charge storage capacity compared to the non-polar faces. Since all ZnO coatings irrespective of orientation exhibit severe capacity fading, further work was restricted to coatings of three types (supplementary figure S1): (i) 002 oriented coatings comprising hexagonal columns with ∼1 μm cross-section, (ii) 101 oriented coatings comprising hexagonal columns with their long axes tilted normal to the substrate, and (iii) unoriented coatings comprising submicron crystallites.

The first discharge curve of coating with 002 orientation yields 558 mAh g^{-1} and 101 orientation yields 566 mAh g^{-1} (supplementary figure S2). A comparable unoriented coating (mass 3.7 mg; thickness 6.6 μm) yields a capacity of 620 mAh g^{-1} (figure 2). In all cases, the first discharge curve exhibits multiple plateaus at 0.26, 0.52, 0.66, 1.28 and 2.54 V, respectively (see for e.g., figure 2a). The various plateau potentials observed by us coincide with those reported by other authors [12], thereby showing that the cells fabricated by us reproduce all the essential features of ZnO anodes. The last plateau at 2.54 V corresponds to the oxidation of Zn → ZnO. This plateau disappears after the second discharge cycle. The capacity fading is evident in the charge–discharge curves (figure 2b) and cycle life data (figure 3a). Similar observations are made in the oriented coatings (supplementary figure S2) as well. To verify if the observed capacity fading is due to the thickness of the deposit, a cohort of coatings were fabricated with a significantly lower mass (2.2 mg; thickness 3.9 μm) (supplementary figure S3) and cycled. The cycle life data (figure 3b) are similar to those of thicker coatings.

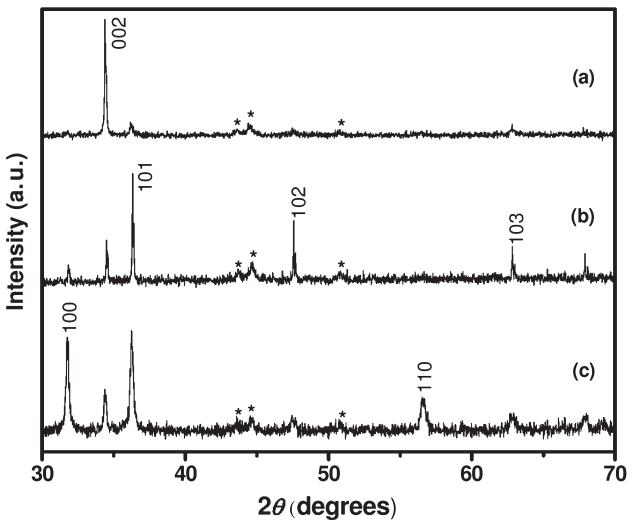

Figure 1. PXRD patterns of (**a**) 002, (**b**) 101 and (**c**) unoriented ZnO coatings. Features marked by ∗ are due to the stainless steel substrate.

From the aforementioned, it is clear that there is no effect of oriented crystallization on the reversible charge storage capacity of ZnO. This is understandable, as in the wurtzite structure, the 100, 010 and 110 planes have comparable surface energies. Consequently, they are equally incident in hexagonal columnar crystallites of ZnO. Additionally, all these planes are non-polar (figure 4) due to which their interaction with the incoming Li^+ ions is expected to be weak in comparison with the polar 001 face. In the specific case of ZnO, the morphology of crystallites in differently oriented coatings is the same. The different out of plane orientations arise merely due to the tilting of the hexagonal columns with respect to the substrate normal [18]. As a result, differently oriented coatings do not expose any new crystal faces with high surface energies other than the 001 face. In this aspect, the electrocrystallization of ZnO is different from that of an oxide such as Cu_2O, wherein differently oriented coatings expose crystal faces [24] with different surface energies. Accordingly, the UV–Vis spectra of differently oriented Cu_2O coatings show different values for λ_{max} [5], but the spectra of differently oriented ZnO coatings look identical (figure 5). If the λ_{max} value (365 nm) is seen as a measure of the band gap, then the band gap (3.4 eV) and consequently, the conductivity

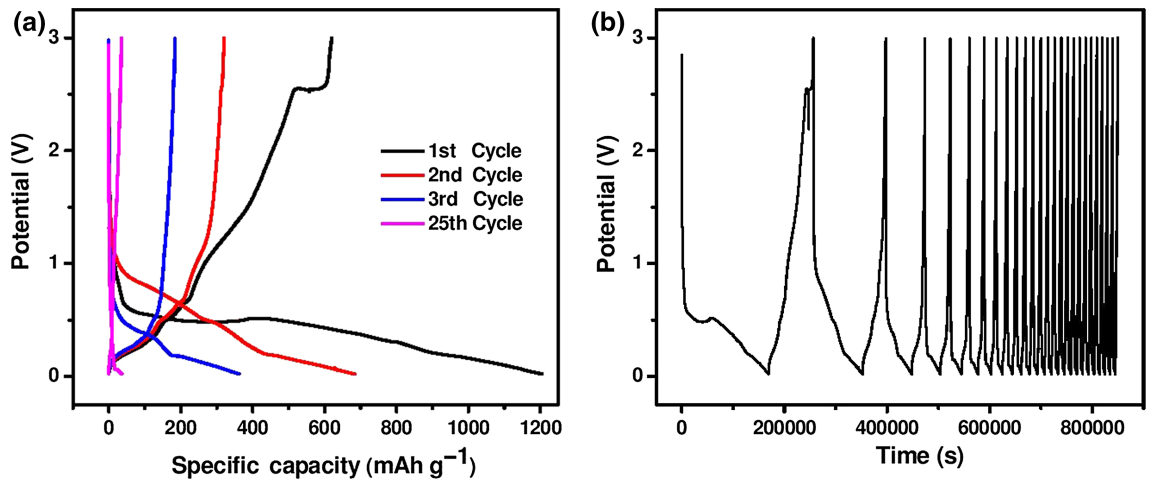

Figure 2. Charge–discharge curves of an unoriented ZnO coating showing (**a**) multiple plateaus in the first discharge curve and (**b**) capacity fading.

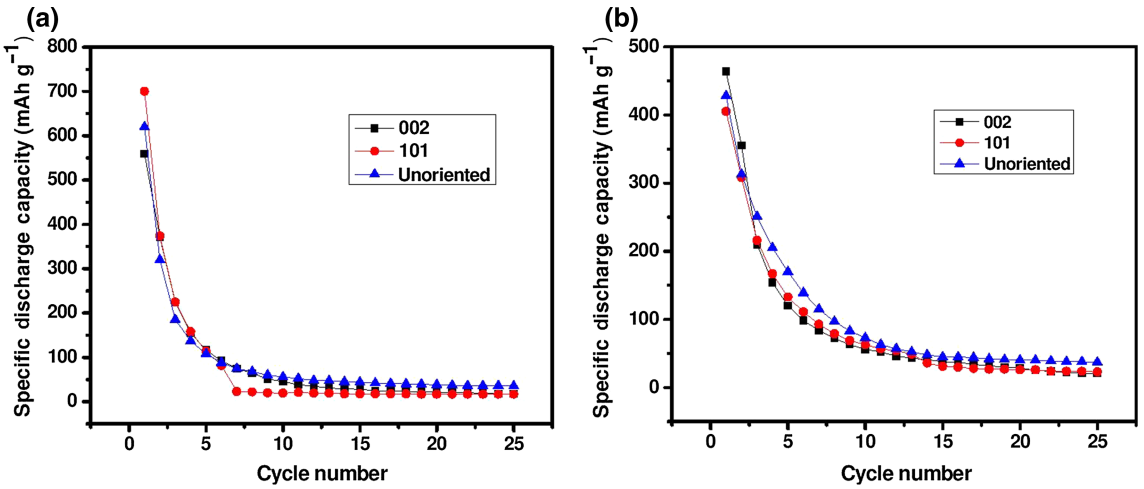

Figure 3. Specific discharge capacities of ZnO coatings with different orientations with (**a**) 3.7 mg mass (average thickness 6.6 μm) and (**b**) 2.2 mg mass (average thickness 3.9 μm).

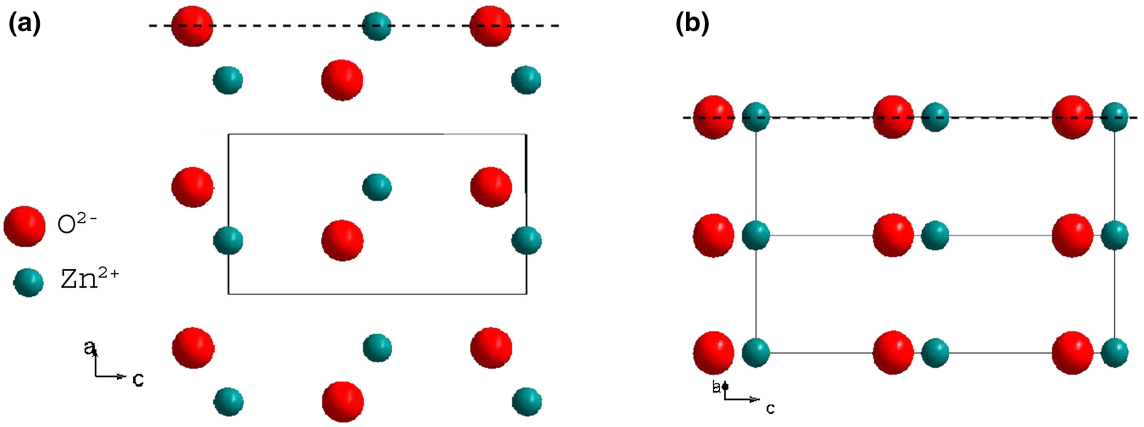

Figure 4. Projections of (**a**) 100 and (**b**) 110 crystal planes of wurtzite ZnO showing their non-polar nature. Dashed horizontal lines identify the crystal planes.

of differently oriented ZnO coatings are comparable to that of unoriented coating.

The spent ZnO anodes were recovered after 25 charge–discharge cycles. Their XRD data show the presence of both ZnO and Zn (figure 6).

TEM images of the spent electrode (see figure 7a for a representative image) reveal submicron columnar structures with spicule-like branches emanating to give Y junctions. The columnar structures are unsurprising as both Zn and ZnO, the end members of the redox cycle crystallize with hexagonal symmetry and tend to grow along the unique 6 axis. In the absence of images of spent ZnO electrodes in the literature, we compare our images with those of other transition metal binary oxide electrodes [1,25]. The following differences are observed:

(1) Typically, the spent electrodes comprise spherical/equiaxed nanoparticles of 5 nm or smaller. In the present case, the crystallites are larger.

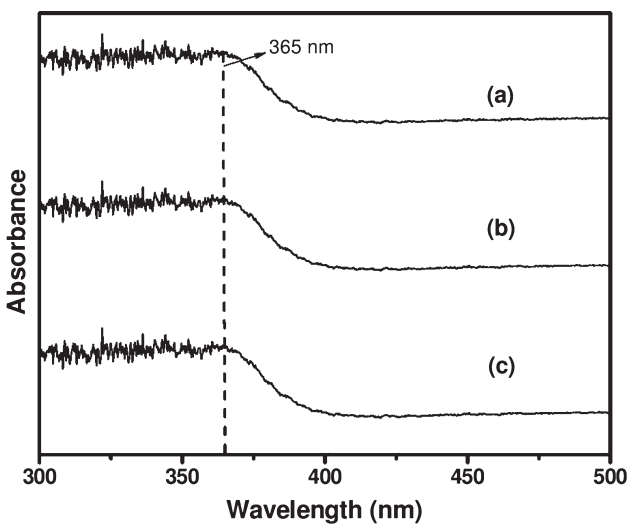

Figure 5. UV/Vis spectra of (**a**) 002, (**b**) 101 and (**c**) unoriented ZnO coatings. The vertical line corresponds to the position of λ_{max}.

(2) The spent electrodes are pseudo-amorphous in nature and yield a ring pattern in electron diffraction. The selected area electron diffraction (SAED) of our electrodes are spotty representative of polycrystalline aggregates. These spots are indexed to 102, 103, 203 planes of ZnO and 002 and 104 planes of Zn (figure 7b).

Reflections due to Li_2O are not observed in this work. This is partly due to the small volume% of Li_2O and partly due to its amorphous nature.

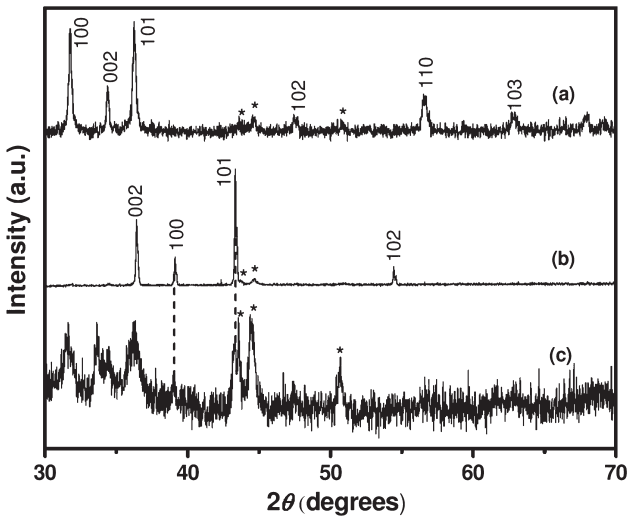

Figure 6. PXRD patterns of (**a**) polycrystalline ZnO and (**b**) polycrystalline Zn compared with the PXRD pattern of the (**c**) ZnO-cycled electrode. Features marked by ∗ are due to the stainless steel substrate.

An earlier investigation into capacity fading of ZnO anodes had shown that metallic Zn accumulates during cycling [11]. The observation of ZnO in the spent electrode was surprising, throwing up the question as to why ZnO anodes suffer severe capacity fading.

To address this issue, impedance measurements were made before cycling and after several (1, 5, 10, 20 and 25) charge–discharge cycles. These are compared with similar data obtained from Cu_2O coatings used for comparison [5], as the latter yielded steady reversible discharge capacities over several cycles.

The impedance spectra (figure 8, supplementary figure S4a and b) show a semicircle in the high frequency range and a linear spike in the low frequency range. The charge transfer resistance R_{ct} is obtained from the diameter of the semicircle. The R_{ct} values for an unoriented ZnO coating is 180 Ω before cycling and remains relatively unchanged until the end of the first cycle (table 1). At the end of 5 cycles, it has increased to 370 Ω and from thereon it remains in the range of 300–400 Ω. These values are much larger than comparable cells comprising Cu_2O anodes, wherein the R_{ct} remains in the range of 30–60 Ω during 30 charge–discharge cycles (table 2). The R_s values remain in the range of 10–20 Ω for all the cells irrespective of the anode, as they were all sealed under similar conditions.

The low frequency spike in the impedance data was used to evaluate the Li^+ diffusion coefficient, D (table 1). It is observed that the D value in unoriented ZnO coatings are an order of magnitude lower than in comparable coatings of Cu_2O up to 5 charge–discharge cycles, by which time capacity has completely faded. The 002 oriented coating has the highest R_{ct} (400–700 Ω) and up to two orders of magnitude lower D^+_{Li} than the Cu_2O coatings.

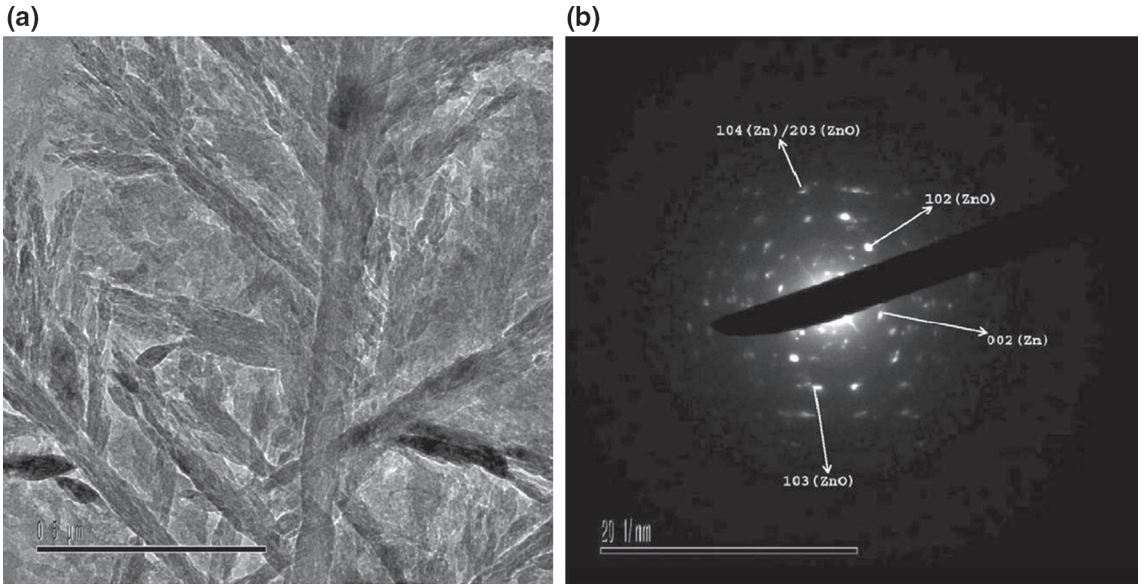

Figure 7. (**a**) A typical TEM image and (**b**) SAED pattern of a ZnO spent electrode.

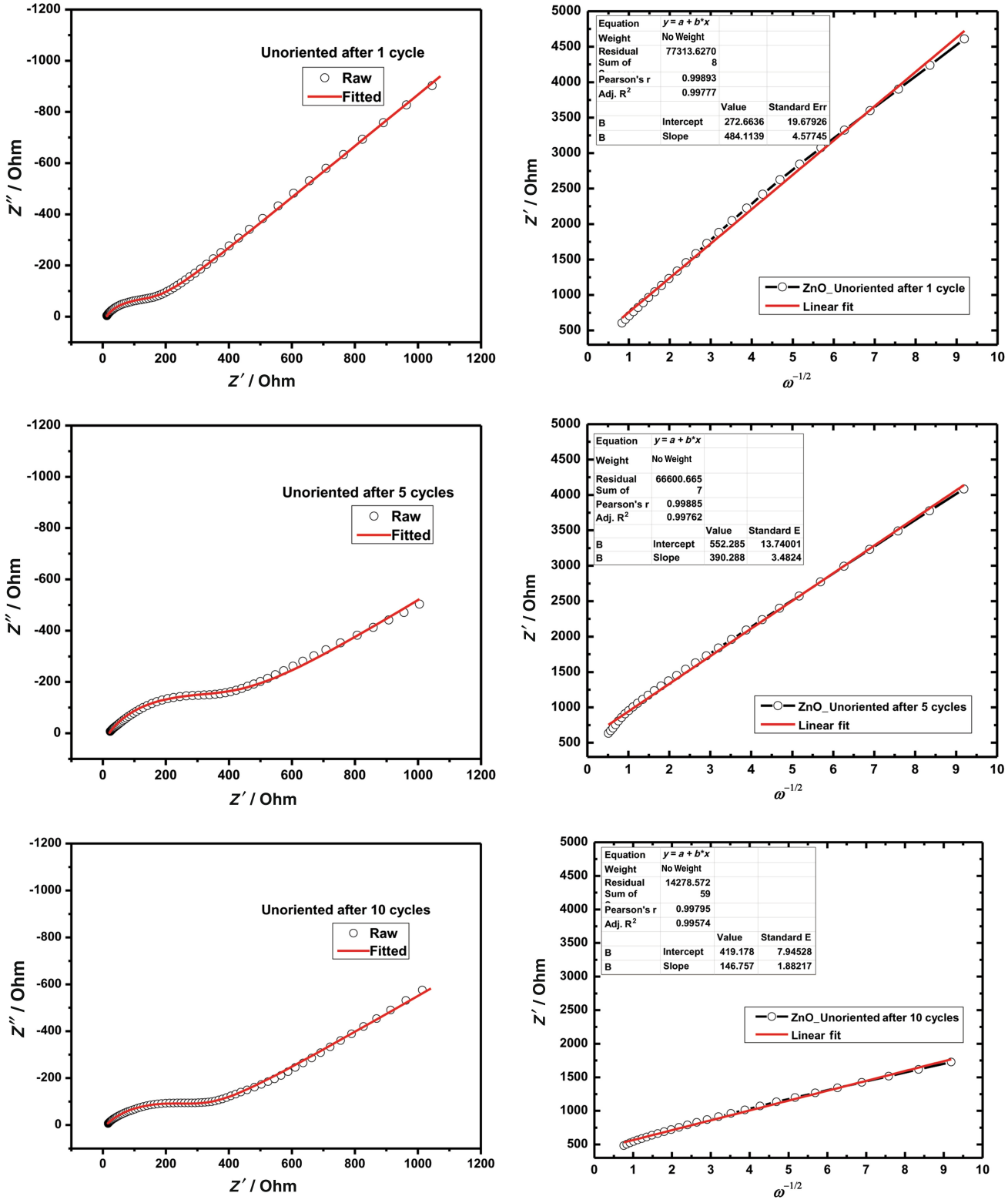

Figure 8. Nyquist impedance plots of unoriented ZnO coatings after 1, 5 and 10 charge–discharge cycles. Alongside are given the corresponding linear fits in the low frequency region.

It therefore appears that the poor performance of ZnO anodes as conversion electrodes is due to (i) high resistivity of the material and (ii) the low diffusion coefficient of Li^+ in ZnO. The latter can be accounted for the fact that ZnO has a close-packed crystal structure. The question then arises as to why close-packed cubic crystals such as NiO and CoO deliver high

Table 1. Results of impedance analysis of the cycled ZnO electrodes.

	Cycle number	R_s	R_{ct}	D^+_{Li} (cm^2 s^{-1})
002	0	33	385	5.675×10^{-15}
	1	24	380	8.950×10^{-14}
	5	45	500	2.706×10^{-13}
	10	55	530	1.684×10^{-13}
	20	60	600	3.101×10^{-13}
	25	55	700	1.860×10^{-13}
101	0	12	1000	1.901×10^{-15}
	1	08	20	9.225×10^{-13}
	5	21	271	8.199×10^{-13}
	10	30	190	1.699×10^{-12}
	20	24	260	1.902×10^{-12}
	25	24	380	9.150×10^{-13}
Unoriented	0	8.4	180	7.522×10^{-14}
	1	12	160	2.402×10^{-13}
	5	20	370	3.700×10^{-13}
	10	10	310	2.640×10^{-12}
	20	15	340	1.480×10^{-12}
	25	15	420	7.496×10^{-13}

Table 2. Results of impedance analysis of the cycled Cu_2O electrodes.

	Cycle number	R_s	R_{ct}	D^+_{Li} (cm^2 s^{-1})
111	0	60	300	5.815×10^{-15}
	1	14.2	36	2.413×10^{-12}
	5	14.7	26	1.936×10^{-12}
	10	14.4	29	2.171×10^{-12}
	20	15	38	1.662×10^{-12}
	30	15.6	44	1.326×10^{-12}
200	0	60	320	1.299×10^{-14}
	1	12	35	3.157×10^{-12}
	5	12.5	84	2.912×10^{-12}
	10	12	36	3.974×10^{-12}
	20	12.3	56	4.825×10^{-12}
	30	13.2	98	2.144×10^{-12}
Unoriented	0	20	1500	2.067×10^{-14}
	1	11	27	3.781×10^{-12}
	5	11.2	28	2.955×10^{-12}
	10	13	63	2.452×10^{-12}
	20	12	55	1.994×10^{-12}
	30	12.5	52	1.717×10^{-12}

capacities in conversion electrodes [1]. This is linked to the fact that neither of these oxides can be prepared in stoichiometric compositions. Black NiO has significant amounts of Ni^{3+} which not only imparts better electronic conductivity to the material, but also generates vacancies in the crystal thereby facilitating Li^+ diffusion. Similar is the case of CoO. On these arguments 'green' NiO is expected to perform worse than 'black' NiO.

4. Conclusions

In contrast with Cu_2O anodes, comparable ZnO anodes suffer severe capacity fading during the charge–discharge process irrespective of their orientation. ZnO is a wide band gap (3.3 eV) semiconductor and has a hexagonal close-packed structure, which results in large charge transfer resistance and low Li^+ ion diffusion coefficient, respectively.

Acknowledgements

We thank the Department of Science and Technology, Government of India, for financial support through the award of a Ramanna Fellowship to PVK.

Electronic supplementary material

Supplementary material pertaining to this article is available on the *Bulletin of Materials Science* website (www.ias.ac.in/matersci).

References

[1] Poizot P, Laruelle S, Grugeon S, Dopant L and Tarascon J M 2000 *Nature* **407** 496
[2] Guo B, Li C and Yuan Z Y 2010 *J. Phys. Chem. C* **114** 12805
[3] Xiang J Y, Tu J P, Huang X H and Yang Y Z 2008 *J. Solid State Electrochem.* **8** 941
[4] Lee Y H, Leu I C, Chang S T, Liao C L and Fung K Z 2004 *Electrochim. Acta* **50** 553
[5] Kiran G K, Penki T R, Kamath P V and Munichandraiah N 2016 *J. Solid State Electrochem.* **20** 555
[6] Noguera C 2000 *J. Phys. Condens. Matter* **12** R367
[7] Rathore N, Rao D V S, Sarkar S K, Sridhara D V and Sarkar S K 2015 *RSC Adv.* **5** 28251
[8] Li H, Huang X and Chen L 1999 *Solid State Ionics* **123** 189
[9] Belliard F and Irvine J T S 2001 *J. Power Sources* **97–98** 219
[10] Liu J, Li Y, Huang X, Li G and Li Z 2008 *Adv. Funct. Mater.* **18** 1448
[11] Hwang H, Kim M G, Kim Y, Martin S W and Cho J 2007 *J. Mater. Chem.* **17** 3161
[12] Pelliccione C J, Ding Y, Timofeeva E V and Segre C U 2015 *J. Electrochem. Soc.* **162** A1935
[13] Liu J, Li Y, Ding R, Jiang J, Hu Y, Ji X *et al* 2009 *J. Phys. Chem. C* **113** 5336
[14] Ahmad M, Yingying S, Nisar A, Sun H, Shen W, Wei M *et al* 2011 *J. Mater. Chem.* **21** 7723
[15] Huang X H, Xia X H, Yuan Y F and Zhou F 2011 *Electrochim. Acta* **56** 4960
[16] Zhang C Q, Tu J P, Yuan Y F, Huang X H, Chen X T and Mao F 2007 *J. Electrochem. Soc.* **154** A65

[17] Wu M S and Chang H W 2013 *J. Phys. Chem. C* **117** 2590
[18] Prasad B E, Kamath P V and Ranganath S 2012 *J. Solid State Electrochem.* **16** 3715
[19] Therese G H A and Kamath P V 2000 *Chem. Mater.* **12** 1195
[20] Zhitomirsky I 2000 *Am. Ceram. Soc. Bull.* **79** 57
[21] Pauporté T and Lincot D 2000 *Electrochim. Acta* **45** 3345
[22] Canava B and Lincot D 1999 *J. Appl. Electrochem.* **30** 711
[23] Prasad B E and Kamath P V 2010 *J. Solid State Electrochem.* **14** 2083
[24] Joseph S and Kamath P V 2007 *J. Electrochem. Soc.* **154** E102
[25] Grugeon S, Laruelle S, Herrerra-Urbina R, Dupont L, Poizot P and Tarascon J M 2001 *J. Electrochem. Soc.* **148** A285